Ferrule-top atomic force microscope

Chavan, D.C.; Gruca, G.L.; de Man, S.P.J.; Slaman, M.J.; Rector, J.H.; Heeck, K.; Iannuzzi, D.

published in
Review of Scientific Instruments
2010

DOI (link to publisher)
10.1063/1.3516044

document version
Publisher's PDF, also known as Version of record

Ferrule-top atomic force microscope

D. Chavan, G. Gruca, S. de Man, M. Slaman, J. H. Rector et al.

Citation: Rev. Sci. Instrum. **81**, 123702 (2010); doi: 10.1063/1.3516044
View online: http://dx.doi.org/10.1063/1.3516044
View Table of Contents: http://rsi.aip.org/resource/1/RSINAK/v81/i12
Published by the American Institute of Physics.

Ferrule-top atomic force microscope

D. Chavan, G. Gruca, S. de Man, M. Slaman, J. H. Rector, K. Heeck, and D. Iannuzzi[a)]
Faculty of Sciences, Department of Physics and Astronomy and LaserLaB, Vrije Universiteit, Amsterdam, The Netherlands

(Received 28 July 2010; accepted 24 October 2010; published online 16 December 2010)

Ferrule-top cantilevers are a new generation of all-optical miniaturized devices for utilization in liquids, harsh environments, and small volumes [G. Gruca *et al.*, Meas. Sci. Technol. **21**, 094033 (2010)]. They are obtained by carving the end of a ferruled fiber in the form of a mechanical beam. Light coupled from the opposite side of the fiber allows detection of cantilever deflections. In this paper, we demonstrate that ferrule-top cantilevers can be used to develop ultra compact AFMs for contact mode imaging in air and in liquids with sensitivity comparable to that of commercial AFMs. The probes do not require any alignment procedure and are easy to handle, favoring applications also outside research laboratories. © *2010 American Institute of Physics*. [doi:10.1063/1.3516044]

I. INTRODUCTION

Since its invention in 1986 (Ref. 1) atomic force microscopy has witnessed an ever increasing popularity. Today, the atomic force microscope (AFM) is considered a unique instrument for its ability to provide surface topology images, force measurements, and information on material properties at the nanoscale. It is thus not surprising to notice that many research groups belonging to both the academic and the industrial environment have been continuously proposing new solutions to improve the performance of their AFMs, from novel imaging modes[2,3] to high speed[4–6] and video rate scanning.[7] In spite of this impressive progress, in most commercially available AFMs the deflection of the cantilever is still detected by means of optical triangulation. Optical triangulation, however, requires a volume of several cm^3, making further miniaturizaton virtually impossible. Furthermore, it does not adapt well to applications beyond research laboratories, where untrained personnel might not be comfortable with the alignment procedure necessary to bring the laser spot on the cantilever before utilization. Alternative detection schemes, like, for example, piezoresistive sensing,[8] can be hardly used in liquid environments. There is thus an evident need of a compact, all-optical probe that overcomes the alignment procedure. In 2006, our group has proposed a new generation of miniaturized devices that may solve this issue: the fiber-top cantilever.[9,10] In a fiber-top probe, the cantilever is carved at the center of the cleaved end of an optical fiber. Light coupled from the opposite side of the fiber can then be used to detect the deflection of the cantilever. The probe is extremely compact (it is machined on a 125 μm diameter fiber), all-optical, and very easy to use (the operator only needs to plug the fiber to the readout system). Unfortunately, fiber-top cantilevers are currently produced by means of a very expensive process (namely, Focused Ion Beam milling[11]). To solve this problem, at the beginning of 2010 we introduced a new approach to fiber-top probes, which now goes under the name of *ferrule-top cantilevers*.[12,13] Ferrule-top cantilevers are obtained by carving a cantilever out of a ferruled optical fiber. Because the dimensions of a ferrule are more than one order of magnitude larger than those of a fiber, the fabrication process can rely on steps that adapt better to cost effective series production. In this paper, we show that it is possible to equip a ferrule-top cantilever with a sharp conical tip for AFM purposes. The ferrule-top probe is then mounted on an extremely compact AFM, where it is used for contact mode imaging in both air and water.

II. FERRULE-TOP PROBE: FABRICATION AND READOUT

Ferrule-top tipped cantilevers are obtained via the fabrication steps illustrated in Fig. 1. The building block is a 2.5 mm × 2.5 mm × 7 mm pierced ferrule made out of borosilicate glass (VitroCom Inc.), with a central bore hole that has a diameter of 127 μm [Fig. 1(i)]. The ferrule is initially mounted on the stage of a ps-laser ablation machine (Optec System with Lumera Laser source), where, following the steps described in Refs. 12 and 13, it is machined into a 220 μm wide, 200 μm thick rectangular ridge [Fig. 1(ii)]. The ablation machine is then used to carve a 50 μm × 50 μm suspended square hole at the end of the ridge and a v-groove on the side of the ferrule [Figs. 1(iii) and 2]. After the ferrule is taken out of the ablation machine, a GeO_2 doped single mode silica fiber (Fibercore Ltd.), equipped with an $\simeq$8 μm high, $\simeq$100 nm radius conical tip,[14] is laid on the v-groove, slid into the rectangular hole, and glued to the ridge [Figs. 1(iv) and 3]. The ferrule is then mounted again on the stage of the ps-laser ablation machine to carve the ridge in the form of a tipped cantilever [Figs. 1(v) and 4]. The length and the width of the cantilever can be controlled within the cutting resolution of the laser ablation system (approximately 5 μm). The thickness of the cantilever is more difficult to control, and is limited to 10 μm reproducibility. Because of those limitations, we generally carve cantilevers that are 2200–2300 μm long, 215–225 μm wide, and 20–30 μm thick, which correspond to spring constants between 8 and 20 N/m and resonance frequencies between 5 and 7 kHz. At

a)Author to whom correspondence should be addressed. Electronic mail: iannuzzi@few.vu.nl.

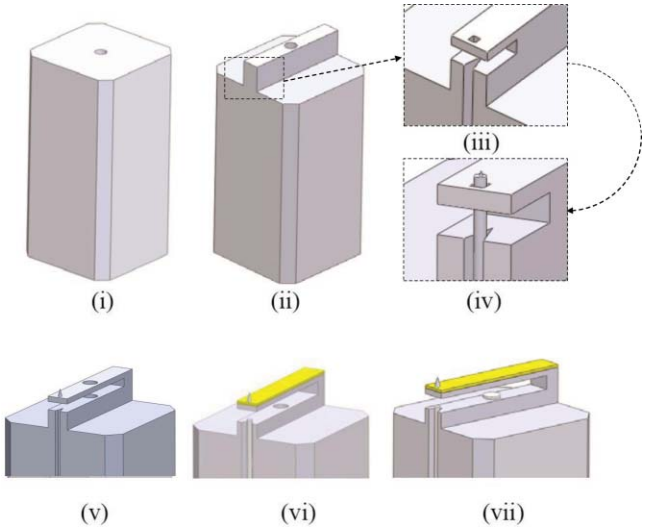

FIG. 1. (Color online) Illustration of the fabrication steps followed for the production of tipped ferrule-top cantilevers (not to scale): (i) the building block is a 2.5 mm × 2.5 mm × 7 mm pierced ferrule made out of borosilicate glass (diameter of the central bore = 127 μm); (ii) the top of the ferrule is machined in a form of a 220 μm wide, 200 μm thick rectangular ridge; (iii) one side of the ridge is machined to host an ≈50 μm diameter fiber; (iv) a ≈50 μm diameter fiber with a conical sharp tip on its end is glued to the ridge; (v) the ridge is further machined in a form of a cantilever (undercut); (vi) a droplet of glue is placed inside the hole at the center of the cantilever, and the probe is coated with a thin gold layer; (vii) a standard single mode optical fiber is inserted into the bore of the ferrule and glued.

the end of the carving process, the residual hole at the center of the cantilever is filled with ultraviolet (UV) curable glue. The probe is then put inside a sputtering system, where it is coated with a 5 nm thick Cr layer followed by a 30 nm thick Au film [Fig. 1(vi)]. Finally, a single mode optical fiber (Corning SMF28-e) is slid into the bore hole of the ferrule and glued [Fig. 1(vii)].

At the opposite end, the fiber is plugged to a commercial optical interferometer readout (LDM1300, Attocube AG) that couples a laser source into the fiber and measures the amplitude of the signal reflected by the head of the probe.[9,15] This signal is the result of the interference between the light reflected at the fiber-to-gap interface, the light reflected by

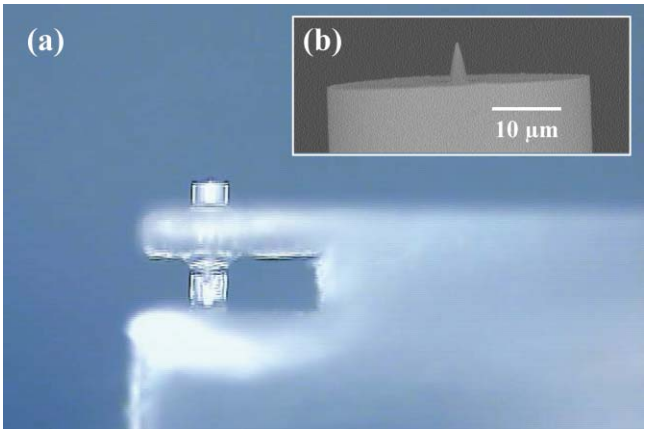

FIG. 3. (Color online) (a) Optical microscope image of the end of the ridge after step (iv) of Fig. 1. (b) Scanning electron microscope image of the sharp tip formed on the GeO_2 doped silica fiber by means of chemical etching in a buffered HF solution.

the gap-to-cantilever interface, and the light reflected at the cantilever-to-metal interface (see Fig. 5), and its amplitude is given by[9,15]

$$W(d) = W_0\left[1 + V\cos\left(\frac{4\pi d}{\lambda} + \varphi_0\right)\right], \tag{1}$$

where d is the separation between the fiber-to-gap and the gap-to-cantilever interfaces, φ_0 is a constant phase shift that only depends on the geometry of the cantilever, λ is the wavelength of the laser ($\lambda = 1310$ nm), and W_0 and V are, respectively, the midpoint interference signal and the fringe visibility. From the signal of the readout system, it is thus possible to remotely sense mechanical displacements of the ferrule-top device.[9,10,12,13]

It is to note that the fabrication procedure presented here is slightly different with respect to that described in Refs. 12 and 13. In the latter, the central fiber is glued before any carving procedure. In this way, however, the surface roughness of the fiber-to-gap and gap-to-cantilever interfaces is determined by the laser ablation process, which cannot provide optically smooth surfaces. The method described here, on the contrary, allows one to rely on optically smooth

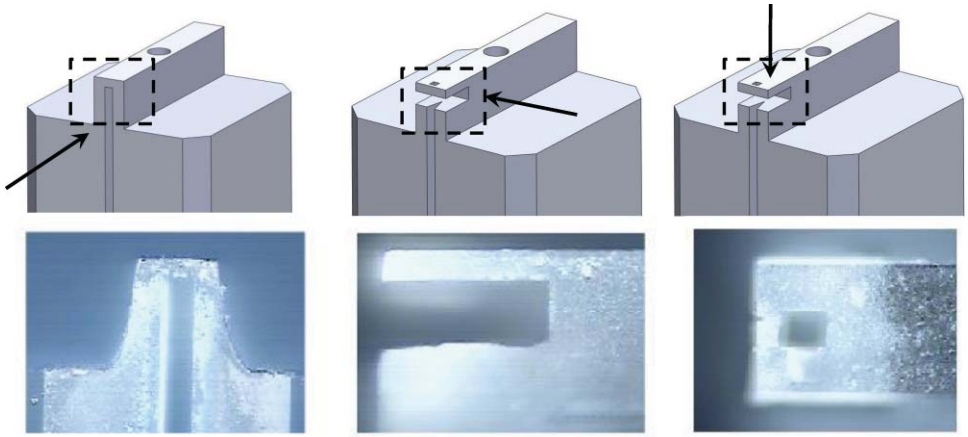

FIG. 2. (Color online) Optical microscope images of the v-groove and of the suspended rectangular hole carved to host a ≈50 μm diameter fiber. The arrows in the drawings indicate the view direction.

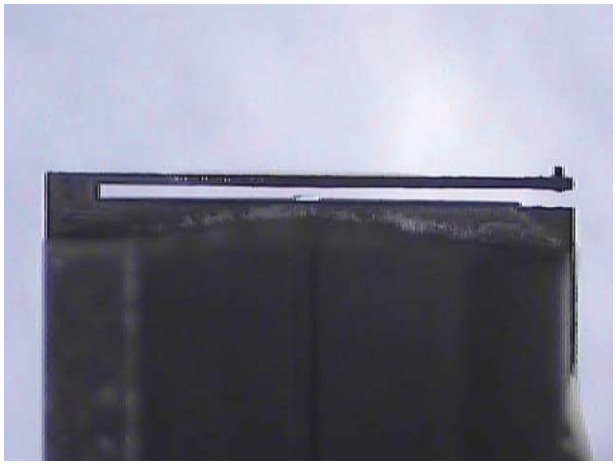

FIG. 4. (Color online) Optical microscope image of a tipped ferrule-top cantilever.

surfaces at all interfaces, increasing the fringe visibility. Thanks to this expedient, it is now possible to systematically achieve an root-mean-square (rms) deflection sensitivity on the order of 0.1 nm (and, thus, 0.3 nN rms force sensitivity for loads applied to the free hanging end of the cantilever) over the 35 kHz bandwidth of the interferometer.

III. FERRULE-TOP AFM: EXPERIMENTAL SETUP

To demonstrate the imaging capabilities of ferrule-top cantilevers, the probe described in the previous section was mounted on the setup sketched in Fig. 5, which consists of a Z-positioner (ANPz51/RES, Attocube AG) with a sample holder, mounted on a 30 μm $\times$ 30 μm range XY-scanner (ANSxy50, Attocube AG) in front of a ferrule-top probe holder equipped with a piezoelectric actuator (AE0203D04F, Thorlabs Inc.). The Z-positioner can be used in stick-slip mode (which moves the sample in discrete steps) or as a

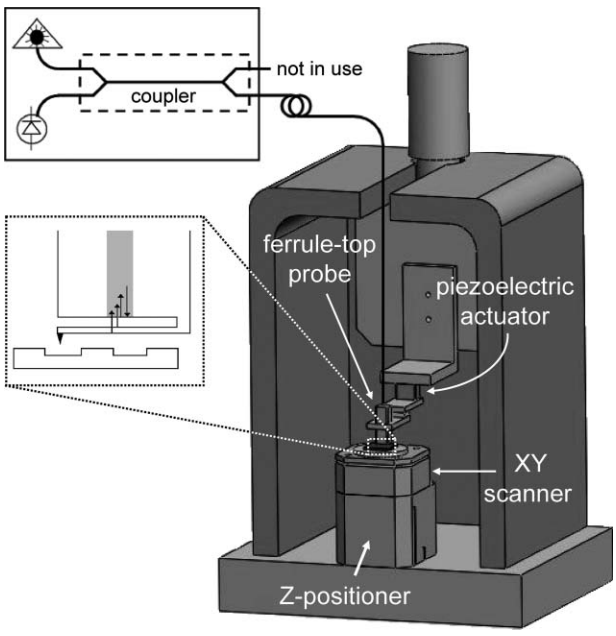

FIG. 5. Schematic view of the ferrule-top AFM.

standard piezoelectric translator (which allows continuous displacement). To facilitate assembly, the probe is glued to a thin 5 mm $\times$ 10 mm iron plate, which is anchored to the holder by means of a small magnet. To reduce acoustic and seismic noise, the entire assembly is mounted on an active vibration isolation stage (Nano-20, Accurion GmbH) housed inside an anechoic box. Thanks to the combined use of ferrule-top technology and compact scanners and positioners, the whole AFM can be contained in a 5 cm $\times$ 5 cm $\times$ 7 cm volume, and, with an accurate design, can be miniaturized even further.

IV. FERRULE-TOP AFM: CONTROL SYSTEM

To obtain a contact mode image, the operator first moves the Z-positioner in a series of discrete stick-slip steps that bring the sample in contact with the sharp conical tip of the ferrule-top cantilever. This procedure is extremely simple, because upon contact, the cantilever undergoes static bending, which is readily detected by the interferometer. Once in contact, the XY-scanner moves the sample underneath the tip to allow raster scan of the area of interest, while a feedback circuit keeps the cantilever deflection constant by moving the sample in the vertical direction, like in standard close loop AFMs.

To close the loop, one could simply fix the set point in correspondence to a position where the cantilever is in quadrature, and then adjust the vertical position of the sample to keep the output signal of the interferometer constant. Following this method, however, the image might be affected by spurious features that are caused by power fluctuations of the laser of the interferometer, which would give rise to signals that would mimic cantilever deflections. This systematic effect can be avoided by using a different feedback method designed to lock the set point not to quadrature but to a maximum or a minimum of interference. In this way, the set point is not defined in terms of absolute voltage output of the interferometer, but as the position where the first derivative of the signal vanishes, which is independent from the output power of the laser.

To lock to a maximum or a minimum of interference, the probe is sinusoidally excited in the vertical direction by means of the piezoelectric actuator of the probe holder at a frequency below the resonance frequency of the cantilever (like in some force modulation techniques already described in the literature).[16] The amplitude of the oscillation is much smaller than the static bending of the cantilever at the set point. Therefore, the tip never loses contact with the surface. This vertical motion is at the heart of the feedback loop that eventually allows one to obtain accurate images of the sample, as explained in detail here below (see Fig. 6).

Let's suppose that, after contact, the Z-positioner, now working in piezoelectric scanning mode, is extended over a length equal to z_+ for which the interference signal is maximum. Let's then assume that the excitation signal of the probe holder is switched on and that, during the XY-scan, the probe initially moves on a flat surface (no change of the output signal). Let's finally imagine that at $t = t_0$ the cantilever is bent upward (or downward) of a small amount d_0 because of the

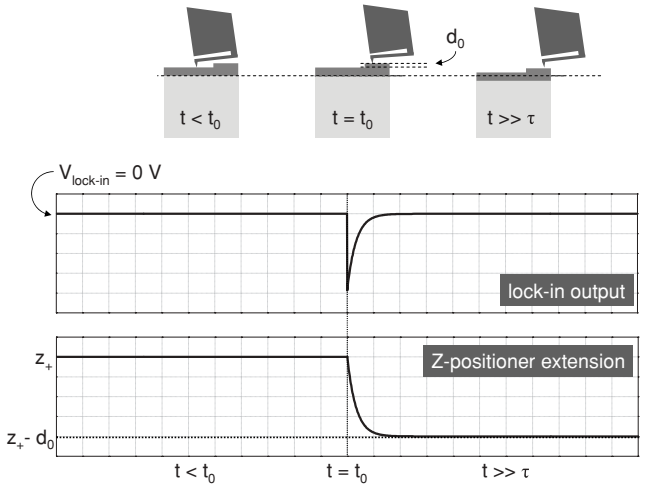

FIG. 6. Schematic view of the working principle that lies at the heart of the high gain feedback loop used in our ferrule-top AFM.

presence of a step in the sample. If one neglects the inertia of the cantilever and the rising time of the readout, the output signal observed is described by [see Eq. (1)]

$$W(t) \approx W_0(1+V) - \frac{1}{2} W_0 V \left(\frac{4\pi}{\lambda}\right)^2 \times (d_0 - z_+ + \delta\cos(\omega t))^2 , \quad (2)$$

whereω and δ are, respectively, the angular frequency and the modulation amplitude of the cantilever in response of the oscillation of the probe holder. From Eq. (2), one can see that W is the sum of one time independent term, one 1ω term, and one 2ω term.

$$W(t) \approx C_0 + C_1(d_0)\cos(\omega t) + C_2\cos(2\omega t) , \quad (3)$$

where the exact expressions of C_0 and C_2 are not relevant for the description of the method, and $C_1(d_0)$ is given by

$$C_1(d_0) = W_0 V \left(\frac{4\pi}{\lambda}\right)^2 (d_0 - z_+)\,\delta. \quad (4)$$

To close the loop, the readout output is sent to a lock-in amplifier locked at frequency ω. The output of the lock-in amplifier is further amplified and sent to the power supply of the Z-positioner. The extension of the Z-positioner at a generic instant t is thus equal to

$$z(t) = \frac{G}{G+1}\left(z_+ - d_0\left(1 - e^{-(t-t_0)/\tau}\right)\right), \quad (5)$$

where G is the loop gain and τ is the loop time constant. From Eq. (5), it is evident that with sufficiently high gain one can accurately reconstruct the image of the sample by looking at the extension of the Z-positioner as a function of the XY-coordinate, and that, in principle, high speed rates can be achieved if the time constant is sufficiently low.

In our instrument, the loop gain and the time constant are set to 80 and 135 μs, respectively. However, we observed that, when driven at high frequencies, our Z-positioner suffers from severe mechanical oscillations that decrease the image quality. For this reason, we have intentionally limited the maximum output current of the amplifier that feeds the

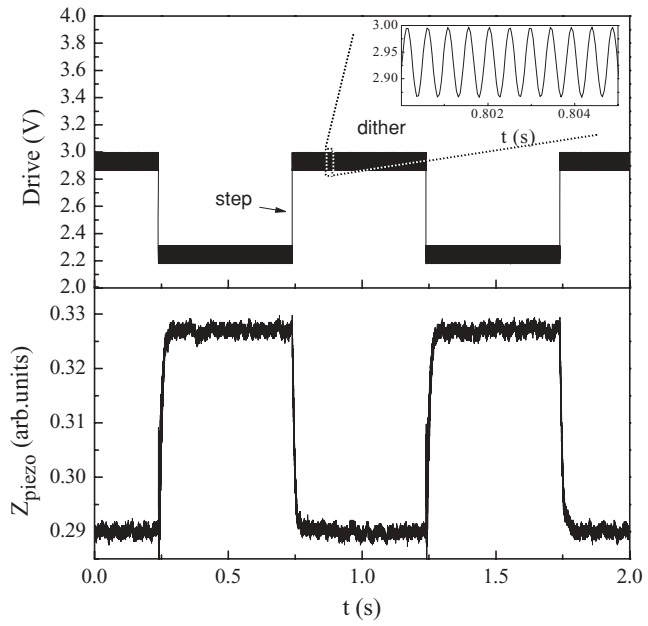

FIG. 7. Movement of the Z-positioner in response to a driving signal that simulates an ≈25 nm sharp step.

Z-positioner. This expedient decreases the scanning speed, but eliminates all the mechanical problems. For example, in Fig. 7 we show the movement of the Z-positioner in response to a driving signal that simulates an ≈25 nm sharp step. From that graph one can see that, indeed, the positioner does not suffer from mechanical oscillations. The response time is, however, limited by a 15 ms long rising time and a 10 ms falling time.

V. FERRULE-TOP AFM: CONTACT MODE IMAGING

In Figs. 8(a) and 8(b) we report images of a 23 nm high calibration grating (NT-MDT TGZ1) obtained in air

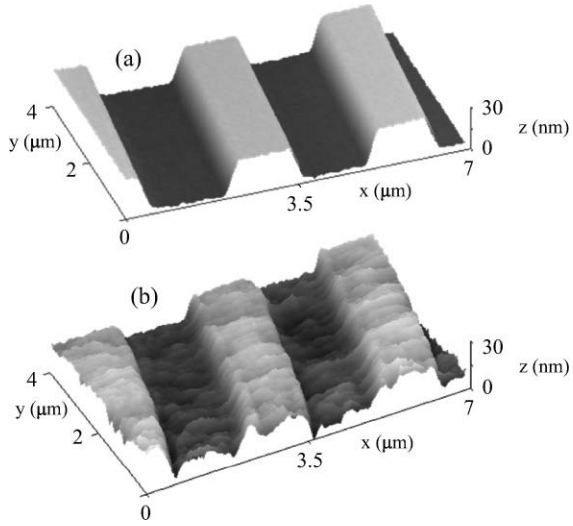

FIG. 8. AFM images of a calibration grating obtained with our ferrule-top AFM in (a) air and (b) water. Images were processed using Gwyddion software with implementation of only standard plane leveling and line correction (see Ref. 17).

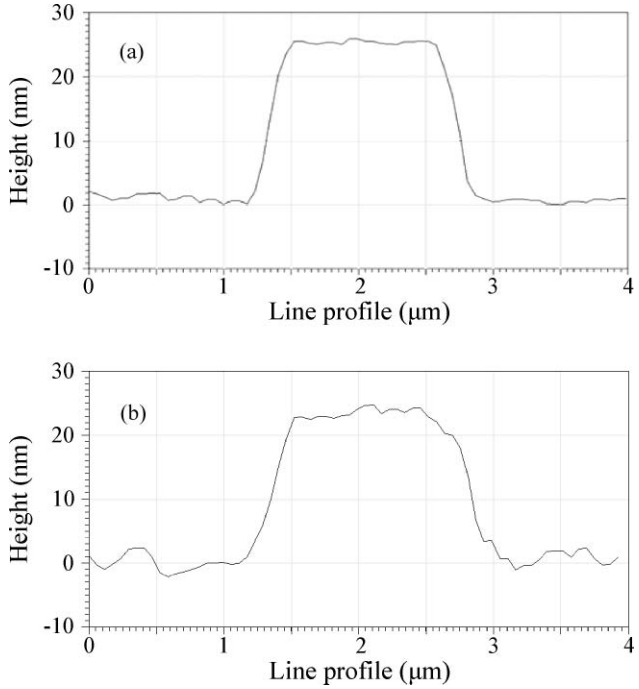

FIG. 9. Line-scan of the AFM images reported in Fig. 8: (a) in air, (b) in water.

and water, respectively. For the latter, the grating was attached to the bottom of a small Petri dish filled with water. Each image covers an area of 7 μm $\times$ 4 μm (resolution 120 pixels $\times$ 70 pixels) with scan time of $\approx$12 minutes. The two images were obtained with two different cantilevers, whose resonance frequencies in atmospheric conditions were independently determined to be 4.9 kHz and 6.2 kHz, respectively. Those values correspond to spring constants of approximately 8 N/m and 15 N/m. Since the feedback mechanism needs, in the worst case scenario, a cantilever deflection of $\lambda/4$ to engage at a maximum or a minimum of interference, the force applied onto the sample during the scan was anyway less than 7.2 μN and 13.5 μN, respectively. The frequency of the vertical oscillation that lies at the heart of the feedback loop was set to 1.1 kHz, with amplitude equal to 15 nm in air and 35 nm in water. From the images reported in Figs. 8(a) and 8(b), it is clear that the instrument can correctly reproduce the shape of the calibration grating. The line-scans reproduced in Fig. 9 further confirm that the quality of the image is comparable to that of commercial AFMs. Indeed, by analyzing the data recorded while the probe was scanning a flat region of the sample, one can see that the rms of the data distribution (that include the effects of vibrations and surface roughness) is equal to 0.5 nm for the image in air and 1.8 nm for the image in water. The slightly higher value obtained in water can be attributed to the presence of small turbulence around the probe, which increases vibrations and, therefore, noise.

VI. CONCLUSIONS

We have fabricated a tipped ferrule-top cantilever for AFM purposes. We have demonstrated that this new kind of probe allows the implementation of very compact, all-optical, triangulation-free AFMs. Thanks to the monolithic design of ferrule-top technology, the user can quickly engage the scanning tip, regardless of the environment in which the sample is immersed. The instrument can then provide high quality images in both air and liquids. We believe that our work paves the way for a new generation of AFMs that are very easy to use, and thus adapt well to utilization in as well as outside research laboratories.

ACKNOWLEDGMENTS

This work was supported by the European Research Council under the European Community's Seventh Framework Programme (FP7/2007-2013)/ERC grant agreement number 201739 and by the Netherlands Organisation for Scientific Research (NWO) under the Innovational Research Incentives Scheme VIDI-680-47-209.

[1] G. Binnig, C. F. Quate, and Ch. Gerber, Phys. Rev. Lett. **56**, 930 (1986).
[2] O. Pfeiffer, R. Bennewitz, A. Baratoff, and E. Meyer, Phys. Rev. B **65**, 161403 (2002).
[3] T. Kasai, B. Bhushan, L. Huang, and C. Su, Nanotechnology **15**, 731 (2004).
[4] Y. Su, A. Brunnschweiler, A. G. R. Evans, and G. Ensell, Sens. Actuators, A **76**, 139 (1999).
[5] G. Schitter, P. Menold, H. F. Knapp, F. Allgower, and A. Stemmer, Rev. Sci. Instrum. **72**, 3320 (2001).
[6] J. K. H. Horber and M. J. Miles, Science **302**, 1002 (2003).
[7] J. P. Howard-Knight and J. K. Hobbs, Appl. Phys. Lett. **93**, 104101 (2008).
[8] R. Pedrak, Tzv. Ivanov, K. Ivanova, T. Gotszalk, N. Abedinov, I. W. Rangelow, K. Edinger, E. Tomerov, T. Schenkel, and P. Hudek, J. Vac. Sci. Technol. B **21**, 3102 (2003).
[9] D. Iannuzzi, S. Deladi, V. J. Gadgil, G. P. Sanders, H. Schreuders, and M. C. Elwenspoek, Appl. Phys. Lett. **88**, 053501 (2006).
[10] D. Iannuzzi, S. Deladi, J. W. Berenschot, S. de Man, K. Heeck, and M. C. Elwenspoek, Rev. Sci. Instrum. **77**, 106105 (2006).
[11] S. Deladi, D. Iannuzzi, V. J. Gadgil, G. P. Sanders, H. Schreuders, and M. C. Elwenspoek, J. Micromech. Microeng. **16**, 886 (2006).
[12] G. Gruca, S. de Man, M. Slaman, J. H. Rector, and D. Iannuzzi, Meas. Sci. Technol. **21**, 094033 (2010).
[13] G. Gruca, S. de Man, M. Slaman, J. H. Rector, and D. Iannuzzi, Proc. SPIE **7503**, PDP07 (2010).
[14] To obtain the tip, we used the method described in T. Pangaribuan, K. Yamada, S. Jiang, H. Oshawa, and M. Ohtsu, Jpn. J. Appl. Phys. **31**, 1302 (1992). The fiber was cleaved and immersed for 360 minutes in a buffered HF solution (NH_4F:HF:H_2O, 7:1:1 volume ratio), where, because of the different etching rate of the cladding and the core, the tip spontaneously forms. Our fibers, however, had a slight dip in the doping profile in correspondence of the most central part of the core. This detail did not allow us to produce tips with a radius smaller than 100 nm. Using a fiber with a uniform doping profile, though, one should be able to systematically produce 10 nm radius tips.
[15] D. Rugar, H. J. Mamin, and P. Guethner, Appl. Phys. Lett. **55**, 2588 (1989).
[16] P. Maivald, H. J. Butt, S. A. C. Gould, C. B. Prater, B. Drake, J. A. Gurley, V. B. Elings, and P. K. Hansma, Nanotechnology **2**, 103 (1991).
[17] See: http://mesh.dl.sourceforge.net/project/gwyddion/user-guide/2009-11-11/gwyddion-user-guide-en-2009-11-11.pdf.